Hydrosphere, 2025
https://doi.org/10.26599/HYD.2023.9380002.V2

Green water: Recycling water resources within the ecosystem-atmosphere network [version 2]

Di Xie[1,2], Yu Zhang[1,2], Deyu Zhong[1,2,3,✉], Guangqian Wang[1,2], Songdong Shao[4]

[1]State Key Laboratory of Hydroscience and Engineering, Tsinghua University, Beijing 100084, China
[2]Department of Hydraulic Engineering, Tsinghua University, Beijing 100084, China
[3]State Key Laboratory of Plateau Ecology and Agriculture, Qinghai University, Xining 810016, China
[4]Key Laboratory of Engineering Software, Dongguan University of Technology, Dongguan 523808, China

ABSTRACT

Green water, temporarily stored in the unsaturated zone of the soil or on the top of vegetation, plays an important role in the natural water cycle and water resource management. Unlike surface water flows, green water recycling has no obvious boundary restrictions and is characterized by long-distance transport. Thus, green water from specific basins can support precipitation not only within the basin but also in neighboring basins and even distant areas. However, water scarcity is typically viewed as a local problem for which management measures at the basin scale seem sufficient without fully considering the interdependence of green water among basins. Limited knowledge of green water recycling could make hydrological water assessments inaccurate. Here, we quantify the global green water recycling network, which links green water as a moisture supply to precipitation and thus contributes to local and remote freshwater resources. Our results show that large basins such as the Congo (green water recycling ratio: 56.6%) are comparatively independent, but still rely to some extent on moisture supplied by other basins (contributing 21.4% of precipitation for the Congo), contradicting the conventional view of basin independence in water management. This illustration of basin interdependence highlights the need for global water governance in the context of the severe global water crisis, and this global green water recycling network provides the basis for a comprehensive assessment of water resources and scarcity under global change.

KEYWORDS

Green water, water scarcity, water management, moisture recycling, evapotranspiration, precipitation.

1 Introduction

Green water refers to the water that is temporarily stored in the unsaturated zone of the soil or on the top of vegetation and eventually returns to the atmosphere as evapotranspiration (Falkenmark et al., 2006). After precipitation falls on the land surface, about 40%–60% (te Wierik et al., 2020) is retained in rivers, lakes and aquifers, known as blue water, while the remainder is in the form of green water in plants and soil. Except for the part of groundwater replenishment through infiltration, green water basically returns to the atmosphere. After the whole process of evapotranspiration entering the atmosphere, traveling with the prevailing winds, and finally falling out as rain, green water realizes terrestrial moisture recycling (Keys et al., 2017). Compared with the watershed-restricted terrestrial blue water cycle, green water recycling is achieved by atmospheric water transport with no obvious boundary restrictions, enabling cross-basin and long-distance transmission of water. Green water recycling is an important process that links the geosphere, atmosphere, biosphere, and anthroposphere, making it critical in the natural water cycle and anthropogenic water resource management.

It has become evident that freshwater scarcity is becoming a threat to the sustainable development of human society in recent decades, with two-thirds of the global population (4.0 billion people) living under conditions of severe water scarcity annually (Mekonnen et al., 2016). This severe situation has already caused competition for water resources between upstream and downstream areas (Flörke et al., 2018). Water scarcity is often assessed using indicators that combine water availability and water demand. The sufficiency of blue water to meet certain demands can be measured with simple scarcity indices (Falkenmark et al., 1989; Alcamo et al., 2002; Oki et al., 2006; Kummu et al., 2010). However, these indicators focus on blue water availability and neglect the important role of green water (Liu et al., 2017). As green water is the most important water resource for food production globally (Rockström et al., 2009), a few indicators have considered green water but only accounted for the part used by crops (Rockström et al., 2009; Gerten et al., 2011; Kummu et al., 2014), which suffer from the drawback of inconsistency and significantly underestimate green water resources (Liu et al., 2017). In the context of the severe global water resource situation, revealing the role of green water in the natural water cycle, and exploring scientific methods for estimating and managing green water resources, is an effective way to solve the water scarcity crisis. Existing studies have used hydrological models, water footprint accounting, and other methods to conduct extensive and in-depth research on global green water about its resource quantity (Mekonnen et al., 2011), consumption (Liu et al., 2009), and function (Falkenmark et al., 2019), etc., but further research is needed on how to fully integrate green water into the water management frameworks.

Globally, more than half of the terrestrial precipitation originates from green water that evaporates over land, with the remainder from evaporation over the ocean (Tuinenburg et al., 2020b). While the importance of evapotranspiration as a moisture source for precipitation has received much attention as a land-atmosphere feedback mechanism (e.g., Schär et al., 1999; Seneviratne et al., 2010; Miralles et al., 2019; Li et al., 2023), it has not received analogous attention in the context of water resources management and research. Moreover, the long-distance transport characteristic of green water implies that human activities, represented by anthropogenic land use change and

✉Address correspondence to Deyu Zhong, zhongdy@tsinghua.edu.cn

large-scale irrigation, will not only affect the blue-green water transformation process in the land surface hydrological process but also impact the precipitation and runoff processes in the downwind area, which in turn has potential impacts on water resources, food production, and even human lifestyle in the downwind region (Sterling et al., 2013; Spracklen et al., 2012; Meier et al., 2021; Hoek van Dijke et al., 2022; Cui et al., 2022). Consequently, the sustainability of water resources should not be considered locally but must be subject to water management on a global scale. In order to link local and global water management measures, researchers need to better understand how these processes interact and how atmospheric vapor fluxes connect different regions (Rockström et al., 2023). This regional atmospheric connection has been investigated by several researchers. For example, Keys et al. (2017) assessed the transboundary moisture recycling dynamics using countries as the unit of analysis; Keys et al. (2018) investigated the extent to which water supplies of megacities are reliant on terrestrial moisture recycling; and Keune et al. (2019) proposed a watershed precipitation recycling network to assess the vulnerability of freshwater resources in Europe. However, the overall pattern and picture of global green water recycling, including not only its physical characteristics but also the limitations of watershed-based water management, is still unclear. This knowledge gap hinders the implementation of comprehensive water resource management worldwide.

In this study, we assess the global green water recycling pattern at continental and basin scales, demonstrating the need to move away from the more conventional basin perspective inherited in hydrological studies in order to effectively address global water security issues. The recycling pattern is quantified based on constructing the spatial connections between evapotranspiration from a source cell and precipitation in a sink cell for each land grid globally using a moisture tracking model from 1980 to 2018, and the independence and interdependence of basin water resources are discussed for each continent.

2 Materials and methods

In this study, the global atmospheric moisture source-sink relationships between global evapotranspiration and precipitation locations are quantified using the Lagrangian moisture tracking model, and the corresponding source-sink relationships are aggregated to the continental and basin scales for each continent.

2.1 Geographical delineation of basins

The analysis in this study is based on the geographical subdivision of basins from the HydroBASINS dataset (Lehner and Grill, 2013). HydroBASINS provides global sub-basin boundaries with 12 hierarchically nested divisions. All HydroBASINS layers were derived from the World Wildlife Fund's HydroSHEDS data (Lehner et al. 2008) based on a grid resolution of 15 arc-seconds. In HydroBASINS, each basin is divided into two sub-basins at locations where river branches converge, provided each branch has an upstream area of at least 100 km^2. For this analysis, only level 1 and level 2 are used. as shown in Figure 1. Level 1 categorizes 9 continental regions including Africa (af), North American Arctic (ar), Central and Southeast Asia (as), Australia and Oceania (au), Europe and Middle East (eu), Greenland (gr), North America and Caribbean (na), South America (sa) and Siberia (si). Level 2 further subdivides each region into large sub-units according to the distribution of river basins.

2.2 Moisture tracking with the UTrack model

Green-water resources refer to the portion of precipitation that remains as moisture in the unsaturated zone and ultimately returns to the atmosphere as evapotranspiration. Therefore, green water flux can be quantified using evapotranspiration datasets. When green water evaporates, it participates in atmospheric circulation in the form of moisture transport. This atmospheric moisture can condense and precipitate in areas that meet the precipitation conditions, while the remaining moisture continues to be transported and undergoes a series of evapotranspiration and precipitation processes. From the perspective of the moisture mass conservation equation, evapotranspiration and precipitation in the middle of the cycle are the moisture source and moisture sink, respectively. Currently, scholars have developed various atmospheric moisture tracking models (Gimeno et al., 2020) to study the global circulation of atmospheric

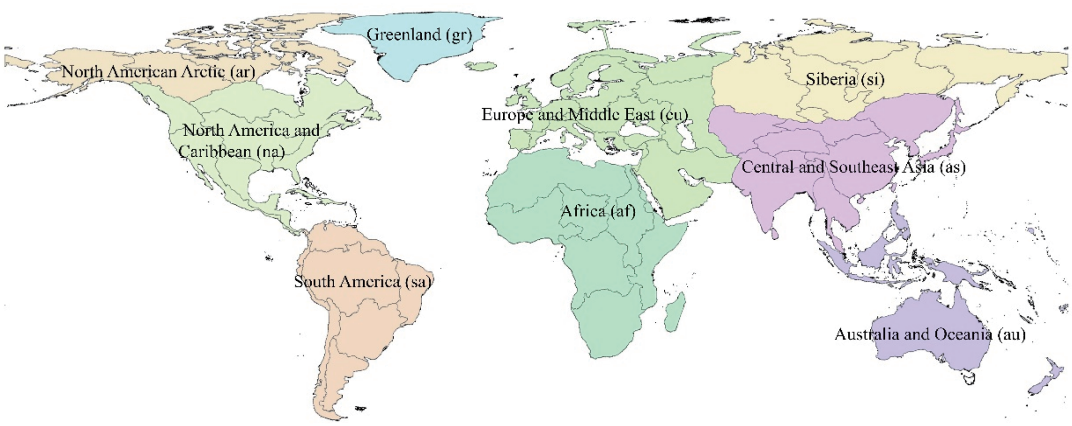

Fig. 1 Geographical subdivision of global basins based on the HydroBASINS dataset. The different colors distinguish the 9 Level 1 continental regions, while the internal lines delineate the Level 2 sub-basins within each continent.

moisture from the perspective of the moisture mass conservation equation. Zhang et al. (2020) conducted a systematic study on the global moisture source-sink relationship and thus pointed out the complex transport and transformation process of global atmospheric moisture. Similarly, the spatial pattern of green water recycling can be investigated using the moisture source-sink relationship. For example, Wang et al. (2023) studied the overall pattern of green water recycling in China and the role of natural and human ecosystems in it based on a Lagrangian moisture tracking model. In this paper, the climatological moisture source-sink relationship was calculated to assess the global pattern of green water recycling. Specifically, a Lagrangian moisture tracking model "UTrack-atmospheric-moisture" (UTrack; Tuinenburg et al., 2020a) was applied to track the atmospheric moisture flux between each pair of grid cells globally. We executed the moisture tracking procedure using ERA-interim reanalysis data (the European Centre for Medium-Range Weather Forecasts Interim Reanalysis data; Dee et al., 2011) with a temporal resolution of 6 h and a spatial resolution of 1 degree as forcing data. Input data includes two-dimensional fields of total precipitation, evaporation, along with three-dimensional fields of specific humidity, wind speed, and wind direction. The Lagrangian analysis tool LAGRANTO (Sprenger et al., 2015) was first run to generate backward air trajectories, releasing air parcels from input data grid cell centers with 10 vertical levels above the surface at 50 hPa intervals at 00, 06, 12, 18 UTC from 1980 to 2018, and tracing the parcels backward in time for 20 days, which is considered sufficient to capture the vast majority of atmospheric moisture sources before the air parcel's moisture becomes fully mixed or precipitates. The output Lagrangian air trajectories were then incorporated into UTrack for atmospheric moisture tracking, with configurations closely following the original model-description papers, in which contributions of particles released at different heights are weighted by the corresponding vertical specific humidity profiles. Further details about the UTrack model and moisture tracking are available in Tuinenburg et al. (2020). The result of moisture tracking provides spatial links between evapotranspiration from a source cell and precipitation in a sink cell for each global grid. It consists of climatological mean moisture fluxes for 1980–2018 with a spatial resolution of 1°. The corresponding source-sink relationships are further aggregated to the continental and basin scales.

2.3 Green water recycling and external contributions

Green water, represented by ET as a quantifiable proxy, can either be recycled locally within the source region or transported to other regions. For each continent, the green water flow can be transported to the interior, to other continents, and to the ocean. When a specific basin is considered, the sink region for green water flow from basin X can be divided into (i) the basin itself, (ii) any other basin Y in the same continental region ($Y \neq X$), or (iii) other undefined sink regions, including land in other continent or ocean and lakes. Similar attribution analysis can be performed for the source of moisture for precipitation. Based on this division, the total evapotranspiration (E_X) and precipitation (P_X) in basin X can be subdivided into three categories, respectively, that is

$$E_X = F(X,X)\cdot E_X + \sum_{Y\neq X} F(X,Y)\cdot E_X + \left(1-\sum_{Y} F(X,Y)\right)\cdot E_X \quad (1)$$

$$P_X = G(X,X)\cdot P_X + \sum_{Y\neq X} G(X,Y)\cdot P_X + \left(1-\sum_{Y} G(X,Y)\right)\cdot P_X \quad (2)$$

where $F(X,Y)$ represents the fraction of green water in basin X that precipitates in basin Y; $G(X,Y)$ represents the fraction of precipitation in basin X that originates from basin Y. Based on the attribution of green water flow and precipitation for basins in each region, the Evapotranspiration Recycling Ratio (ERR) and Precipitation Recycling Ratio (PRR) can be calculated:

$$\mathrm{ERR} = \frac{F(X,X)\cdot E_X}{E_X} \quad (3)$$

$$\mathrm{PRR} = \frac{G(X,X)\cdot P_X}{P_X} \quad (4)$$

and an External Basin-sink Evapotranspiration Ratio (EBER) that defines the green water contribution of basin X to other basins in the same region, and a corresponding External Basin-source Precipitation Ratio (EBPR) that defines the precipitation contribution of other basins in the same region to X can be calculated:

$$\mathrm{EBRR} = \frac{\sum_{Y\neq X} F(X,Y)\cdot E_X}{E_X} \quad (5)$$

$$\mathrm{PBRR} = \frac{\sum_{Y\neq X} G(X,Y)\cdot P_X}{P_X} \quad (6)$$

Therefore, the ERR and PRR describe the self-reliance characteristics of the green water in basin X, and the EBER and EBPR describe the inter-dependence between basin X and other basins in the same region. Based on these two components, the green water contribution to external regions globally (External Region-sink Evapotranspiration Ratio, ERER) and the precipitation ratio originating from external regions (External Basin-source Precipitation Ratio, ERPR) in basin X can be calculated as the difference between 1 and the sum of the corresponding ratio concerning the basin X and other basins in the same region.

3 Results

3.1 Green water recycling and exchange among continents

The analyses of the green water recycling and exchange features are first conducted for 9 continental regions in HydroBASINS. Based on the green water flows between regions, a green water recycling network can be constructed, as illustrated in Figure 2 in the form of a chord diagram. 9 continental regions are represented by different colored bars: South America (red), Africa (yellow), Central and Southeast Asia (blue), North America and Caribbean (light green), Europe and Middle East (orange), Australia and Oceania (brown), Siberia (dark blue), North American Arctic (grey), Greenland (dark green). Also, the entire ocean and sea are shown in light blue, but the self-recycling moisture for it is not shown in the diagram. The arc of each bar is proportional to the sum of the contributed and received volumes of water, and the chords show the flow of atmospheric moisture from the source region to the sink region.

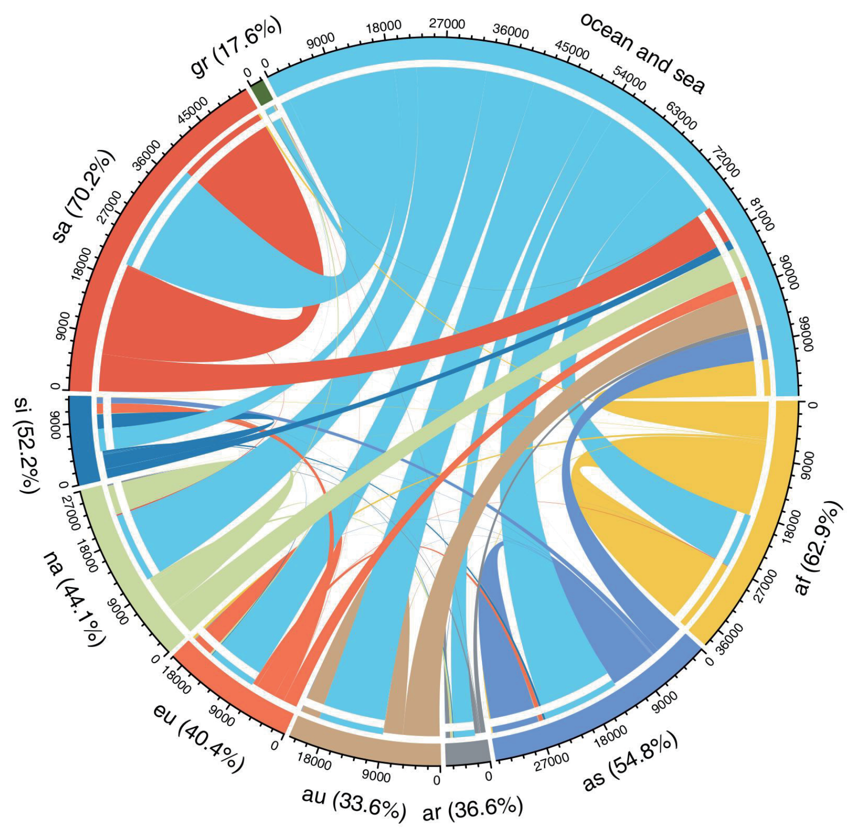

Fig. 2 Global green water exchange network for the 9 continental regions in 1980–2018. Each bar in different a color represents a source region and the chords between regions illustrate the green water flow between evaporation in the source region and precipitation in the sink region (billion m³/a), based on the ensemble mean of moisture tracking results. Flows are illustrated from the source region (represented by one gap between the region bar and the flow line) to the sink region (represented by two gaps between the region bar and the flow line). The numbers in parentheses in the region labels are the self-cycling ratios for each region. Region acronyms: af, Africa; ar, North American Arctic; as, Central and Southeast Asia; au, Australia and Oceania; eu, Europe and Middle East; gr, Greenland; na, North America and Caribbean; sa, South America; si, Siberia.

Figure 2 shows that, at the continental scale, the green water in each region is mainly transported to the region itself and the surrounding ocean, while the region-to-region transport is at a smaller order of magnitude compared to self-recycling and land-sea interaction. As for self-recycling, more than 50% of green water goes back to the source region in South America (ERR is 70.2%), Africa (62.9%), Central and Southeast Asia (54.8%), and Siberia (52.2%), and the green water flow makes a contribution for local precipitation in these regions with the PRR of 44.9%, 56.7%, 35.2%, and 26.9%, correspondingly. In contrast, a relatively low percentage of green water is recycled locally in North America and Caribbean (44.1%), Europe and Middle East (40.4%), North American Arctic (36.6%), and Australia and Oceania (33.6%), especially in Greenland (17.6%), where most of the green water is transferred to external regions. There is an apparent reliance on ERR and PRR on the region size as the recycling ratio of moisture tends to increase with the area (van der Ent et al., 2011). As a result, usually the large continents are projected to be more independent in green water recycling than small regions. Also, large volumes of green water in these regions are transported to the surrounding ocean and sea under the impact of wind, especially in Greenland, Australia and Oceania, where more than half of the green water (68.2% and 65.0%) goes out to the ocean. This proportion of green water that flows to the ocean is also quite high in other regions, with values of 45.0%, 45.0%, 35.4%, 33.2%, 31.4%, 28.8%, and 27.9% in North American Arctic, North America and Caribbean, Central and Southeast Asia, Siberia, Africa, South America, and Europe and Middle East. In addition, external oceans and seas play an even more significant role in the precipitation contribution to land, with more than half of the precipitation coming from ocean evaporation for most of the regions, such as Australia and Oceania (76.9%), Greenland (75.3%), North American Arctic (71.4%), North America and Caribbean (68.2%), Europe and Middle East (65.3%), Central and South-

East Asia (58.2%), and South America (54.1%), while this ratio is relatively low in Africa (42.6%) and Siberia (41.1%). As for the moisture transport between continental regions, the results show that the green water exchange between these regions is not significant as the global land is separated by vast oceans so that only a small amount of atmospheric water vapor can travel long distances to reach other continents. The observed green water recycling network reflects complex interactions between atmospheric circulation, regional climate, and land cover. These insights into green water recycling patterns could inform global water resource management strategies, especially in the context of climate change, by identifying regions that are likely to experience more substantial changes in water availability due to shifts in recycling dynamics.

3.2 Green water recycling pattern of basins

To further clarify the interior structure of green water in the 9 regions, we calculated the green water recycling and exchange patterns in the level 2 basins for each region. The self-supply characteristics of green water resources are shown as ERR and PRR, while inter-dependence characteristics of green water between basins are depicted as EBER and EBPR.

In terms of green water independence, a proportion of precipitation in any given basin will originate from atmospheric moisture produced by evapotranspiration within the basin as shown in Figures 3(a)-3(b) with the ERR and PRR. For South America, the values of basin-scale ERR range from 11.8% (Salado) to 61.5% (Amazon), which means that only 11.8% of moisture from the Salado basin supplies its precipitation, while the Amazon basin is more self-dependence as 61.5% of its evapotranspiration goes back to the local, which supplies 37.2% of its precipitation. As for Africa, the Congo basin features the highest recycling ratio in this region, with 56.6% of its green recycled back to the local and making a contribution of 46.0% to the local precipitation. While the low self-reliance on green water occurs in the Sahara with an ERR value of 15.2%. In central and southeast Asia, the high self-dependence area locates in Ganges and Indus basin with a high ERR of 44.6% and a PRR of 27.7%. Also, the Yangtze and Yellow River basins and Northeastern Tibetan Plateau have a relatively high self-recycling ratio (43.6% and 41.4%), providing 27.3% and 40.5% of their local precipitation correspondingly, while the self-recycling ratio of green water is relatively low in Japan and Mongolia with the value of 7.9% and 12.9%, respectively. In North America

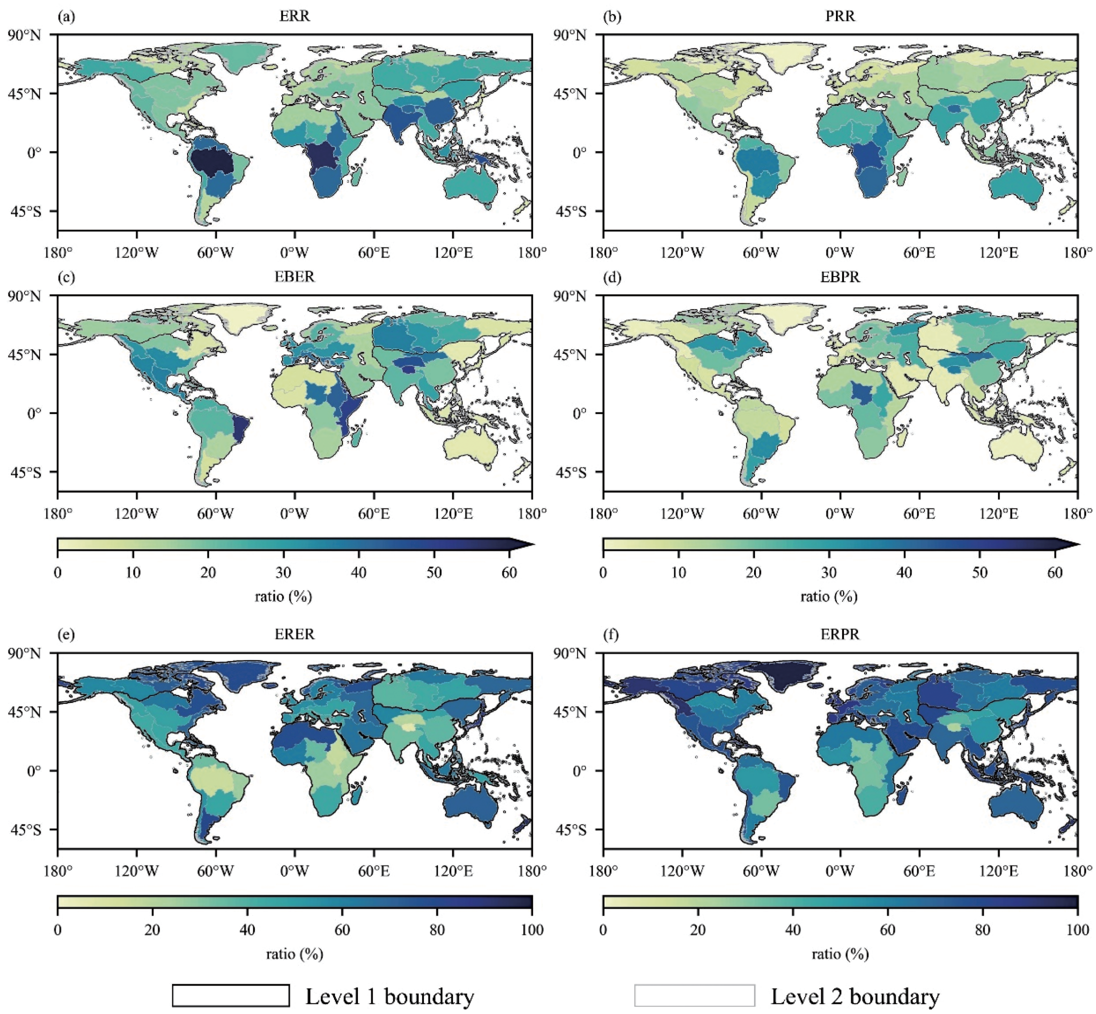

Fig. 3 Green water recycling pattern for level 2 basins in each level 1 region, including the ratio of green water transmitted to the basin itself (ERR, a), the precipitation originating from the basin itself (PRR, b), the green water transmitted to other basin in the same main region (EBER, c), the precipitation originating from other basins in the same main region (EBPR, d). The solid black line delineates the boundary of level 1 regions and the solid grey line delineates the boundary of level 2 basins.

and Caribbean, the ERR and PRR are relatively low (<25.0%) in all basins compared to other regions, and the highest ERR (21.7%) exists in the Colorado basin, where local green water supplies 17.2% of the precipitation. Also, the ERR and PRR in all the subregions in Europe are relatively low (⩽25.0%) and the most notable green water self-recycling (20.4%) exists in the Danube and Dnieper basin. In the Siberian region, the green water recycling ratio of the basins is in a smaller range from 12.5% (Altai) to 27.6% (Lena), and the Ob, Yenisey and Kolyma basins have similar ERR with values of 25.4%, 25.3% and 24.7%, respectively. These figures imply that some basins are highly dependent on local green water to maintain their precipitation, especially for large basins in the tropics such as Amazon, Congo and Ganges. Besides, some inland basins are also characterized by a high self-recycling ratio due to their unique topography, typified by the Northeastern Tibetan Plateau.

Nonetheless, these results show that most basins are far from being individual systems but rather have strong green water exchanges with surrounding basins. Figures 3(c)-3(d) show, for each basin, the fraction of green water that supplies precipitation in other basins (EBER) and the local precipitation that is supplied by evapotranspiration from other basins (EBPR), thus illustrating the degree of inter-dependence of basins in each region. For South America, the San Francisco basin has a higher EBER than other basins with a value of 54.7% under the impact of the prevailing trade winds. Also, 33.7% and 29.2% of the precipitation in the Parana and Salado basin, respectively, is supplied by green water from other basins. As for Africa, high EBER exists in Juba-Shabelle (49.7%), Nile (42.4%), and Lake Chad (39.6%), while 27.5% and 43.8% of the precipitation in the Nile and Lake Chad basin originate from the surrounding basins, which is also related to the direction of the trade winds. In central and southeast Asia, green water from inland regions including Northeastern Tibetan Plateau, Tarim, and Mongolia is largely transported to surrounding basins with a ratio of 51.2%, 45.6%, and 39.0%, respectively. In addition, 37.2%, 32.6%, and 40.0% of the precipitation in these regions originates from other basins. These inland basins have weak interactions with the ocean and are therefore characterized by relatively strong green water exchange with surrounding basins except for self-recycling. In North American and Caribbean, the cross-basin exchange is generally strong in extensive eastern and southern areas with an average EBER of 34.4%, including Rio Grande (36.5%), Colorado (35.2%), Mississippi (33.9%), Frasier and Columbia (32.1%). Besides, the precipitation in Nelson and St Lawrence largely depends on green water from other basins with EBPR at the value of 31.6% and 30.7%. This pattern results from the predominant westerly winds. In Europe, large volumes of green water are transported to other basins in the Mediterranean region (40.8%), Loire (32.7%), Danube and Dnieper (32.0%), while the high EBPR exists in the Barents-Kara Sea region (31.1%) and the Volga basin (24.8%), which is also related to the direction of the westerly winds. In the Siberian region, the green water in Altai and Ob is transported to other basins with high ratios of 40.2% and 36.4%. As for EBPR, 27.0% of Altai's precipitation originates from surrounding regions while only 2.4% of Ob's precipitation is supplied by surrounding basins, which means that Ob basin is an important green water supplier for other basins in Siberia. Overall, the cross-basin exchange is usually controlled by the predominant wind direction and speed so that high EBER tends to exist in the upwind basins while high EBPR appears in the downwind regions.

In addition to the self-recycling and the cross-basin transport of green water, the exchange between basins and external regions especially the ocean and sea is also significant, which can be depicted with the value of ERER and ERPR for each basin, as shown in Figures 3(e)-3(f). For example, in South America, the Salado basin has a higher ERER than other basins with a value of 80.5%, while over 70% of precipitation in the Andes (ERPR is 75.6%) and San Francisco (74.7%) basin originates from the ocean and sea. These coastal basins are more strongly influenced by the surrounding oceans, and watersheds with substantial green water outflows to the ocean often depend on green water replenishment from adjacent basins.

3.3 Green water exchange pattern of basins

The contribution of a basin to the moisture supply for precipitation to other basins, as illustrated in Figure 3(c), can be decomposed into the moisture flows to individual basins, so green water flows between any two basins in six major regions are further quantified and shown in Figure 4. For South America, the green water flows between the Amazon and Parana basins (1,308 billion m^3/a) are much greater than any other cross-basin green water exchanges globally, implying that the Amazon rainforest is an important source of precipitation for the Parana basin, supplying 25.7% of its total precipitation. Also, relatively large green water flows exist from San Francisco to Amazon (706 billion m^3/a) and Parana (286 billion m^3/a), from Amazon to Andes (316 billion m^3/a), and from Parana to Salado (225 billion m^3/a), showing a general north-south transfer trend. Besides, the green water exchange between Caribbean Sea area and Amazon is intense, with amounts of 625 and 478 billion m^3/a, respectively. As for Africa, the Congo Basin is characterized by an intense exchange with the surrounding basins. On the one hand, it supplies a relatively large volume of green water to Orange (313 billion m^3/a), Nile (263 billion m^3/a) and Niger (226 billion m^3/a). On the other hand, green water from surrounding basins is also transmitted to the Congo basin, including Nile (572 billion m^3/a), Juba-Shabelle (519 billion m^3/a), and Orange (349 billion m^3/a). A relatively large green water transport can be detected from Juba-Shabelle to Nile basin (285 billion m^3/a). In central and southeast Asia, large cross-basin green water flows exist from the Mekong River basin to Yangtze and Yellow River basin (601 billion m^3/a), from Yangtze and Yellow basin to the Amur basin (426 billion m^3/a), from Ganges basin to Yangtze and Yellow basin (336 billion m^3/a) and Mekong basin (301 billion m^3/a), showing an overall trend of from southwest to northeast. Besides, the green water exchange conceding inland basins such as Mongolia and Tarim Basin are at relatively small volume but a west-to-east transport can be detected. In North America and Caribbean, there are significant green water transports from Mississippi to St Lawrence (472 billion m^3/a) and Nelson (257 billion m^3/a) basin, from Rio Grande to Mississippi (292 billion m^3/a), and from Colorado to Mississippi (292 billion m^3/a), which shows the characteristics of southwest-northeast green water transport. In Europe, large cross-basin green water flows exist from the Danube basin to the Volga basin (200 billion m^3/a) and Barents-Kara Sea areas (130 billion m^3/a), from the Mediterranean Sea areas to Danube (161 billion m^3/a), from Euphrates to Volga (122 billion m^3/a), and from the Loire to Baltic Sea surrounding areas (104 billion m^3/a), showing an overall trend from western Europe to central Europe. In Siberian region, there are significant green water transports from the Ob basin to the Yenisei (288 billion m^3/a) and Lena (133 billion m^3/a) river basins, from Yenisei to Lena basin (159 billion m^3/a), from Lena to Kolyma basin (118 billion m^3/a). The cross-basin transfer of green water is characterized by a west-to-east trend, which is also consistent with the distribution of the total green water supply being high in the west and low in the east.

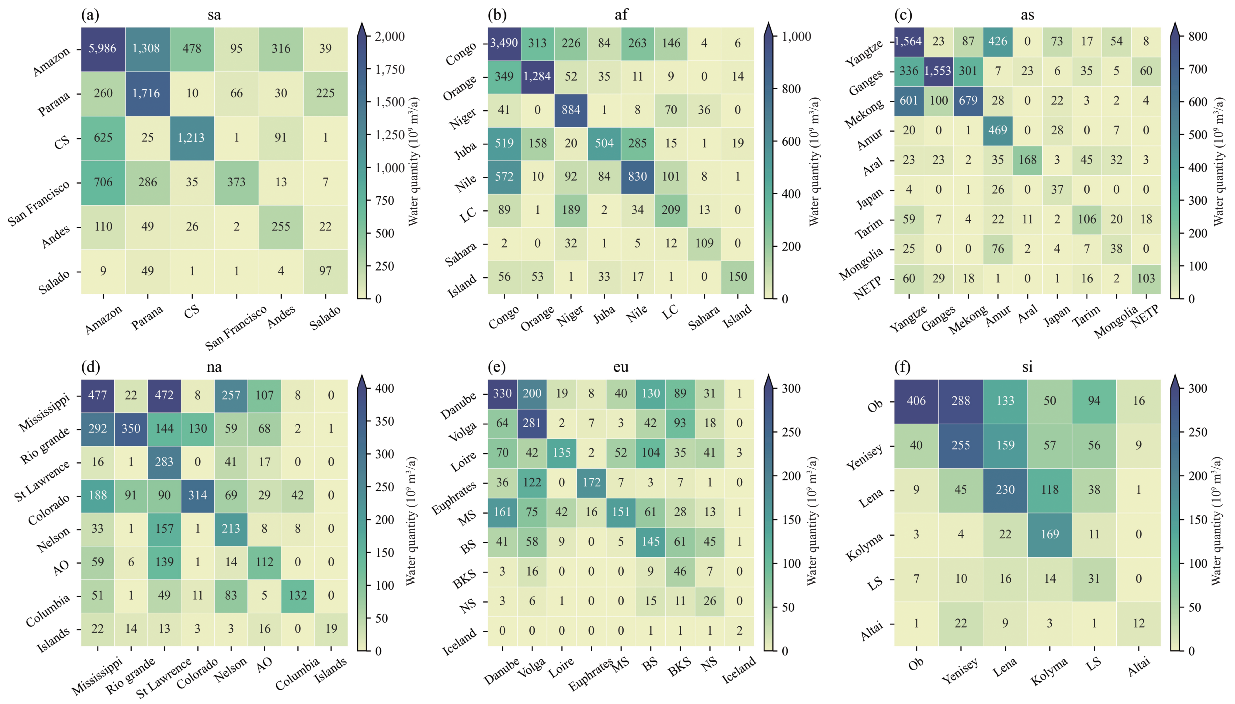

Fig. 4 Quantity of green water exchange between basins in six major regions including (a) South America (sa), (b) Africa (af), (c) Central and Southeast Asia (as), (d) Europe and Middle East (eu), (e) North America and Caribbean (na), and (g) Siberia (si). The *X*-axis and *Y*-axis represent the sink region and source region for green water transport, respectively. The basins are ranked by the total green water quantity they supply and are labeled based on the largest river in each basin or geographical location. Several abbreviations are used for simplicity including CS: Caribbean Sea area; LC: Lake Chad area; NETP: Northeastern Tibetan Plateau; AO: Atlantic Ocean area; MS: Mediterranean Sea area; BS: Baltic Sea area; BKS: Barents-kara Sea area; NS: Norwegian Sea area; LS: Laptev Sea area.

Apart from the detected strong cross-basin green water flow and the overall green water transport trend in each continent, Figure 4 also allows the identification of green water recycling network structures, that is, moisture pathways and their cascading effects. For example, in central and southeast Asia, a large percentage of green water is transmitted from the Ganges basin to the Mekong basin to support local precipitation; this precipitation is partly returned to the atmosphere through evapotranspiration and supplies moisture for precipitation over the Yangtze and Yellow basin, which in turn contributes to the precipitation over the Amur basin, The existence of such cascading moisture recycling has a significant impacts on the moisture transport (Zemp et al., 2014) and even enables the propagation of extreme drought events (Zemp et al., 2017), which further emphasizes the necessity of creating multi-basin integrated water management measures to tackle continental to global water governance.

3.4 Key basins in the global green water recycling

As illustrated above, the basins with substantial green water quantity tend to play the most pivotal roles within their regions, designating them as key basins in green water recycling. To further analyze the features of these key basins, the evapotranspiration, precipitation, and water availability are subdivided as we described in section 2.3 for the top 10 basins that supply the largest volumes of green water globally (Figure 5), ranked as Amazon (9,738 billion m^3/a), Congo, Parana, Yellow and Yangtze, Ganges, Orange, Caribbean Sea areas, Niger, Mekong, Mississippi (2,576 billion m^3/a). As the main suppliers of green water, they also receive large amounts of water globally ranging from 3,106 billion m^3/a (Orange) to 16,097 billion m^3/a (Amazon), as shown in Figure 5(a). However, an imbalance between evapotranspiration and precipitation widely exists, which affects the net water availability (P-E).

Specifically, the Amazon basin is characterized by a substantial water availability increase (6,359 billion m^3/a), which is significantly greater than other basins (1,293 billion m^3/a on average) (Figure 5(b)), as the external ocean areas provide a significant amount of water for precipitation in the Amazon region (8,400 billion m^3/a), much more than the green water provided by the Amazon region to the external areas (1,516 billion m^3/a). Therefore, although the Amazon acts as a supplier of green water to other basins in South America (525 billion m^3/a), the water availability increases because of the compensation from the ocean and sea. The same features apply to the water availability change in the Ganges (a net gain of 2,722 billion m^3/a water from external regions), Caribbean Sea surrounding areas (2,283 billion m^3/a), Mekong (2,217 billion m^3/a) and Mississippi (852 billion m^3/a) basins but with relatively small volumes of water exchange. Simultaneously, some basins including the Congo, Yellow and Yangtze, and Niger, experience a net gain of water from both the surrounding basins and external ocean areas. For example, in the Yellow and Yangtze River basin, the precipitation received from other basins (1,128 billion m^3/a) exceeds the supply of precipitation to other basins (687 billion m^3/a). Beyond that, this basin receives more precipitation from external regions (3,042 billion m^3/a) than it supplies (1,340 billion m^3/a), resulting in a total net gain of freshwater (2,143 billion m^3/a). Similarly, the Congo and Niger receive a net gain of 1,422 billion m^3/a and 509 billion m^3/a of water, respectively, from the combined contribution of surrounding basins and external ocean areas. Different from the basins analyzed above, Panama receives a net volume of 1,126 billion m^3/a green water from basins in the same region, acting as a moisture sink in the South American continent, but supplies more green water to oceans (1,937 billion m³/a) than it receives (1,665 billion m³/a). As for the Orange basin, the net water exchanges with surrounding regions (a net gain of 67 billion m³/a) and external regions (a net loss of 92 billion m³/a) is in relative equilibrium, making the basin-scale water availability a stable state. These results show that cross-basin green water exchange can cause a water availability deficit in certain regions while this impact may be compensated by the moisture supply from the ocean. Also, some basins rely on the net green water supply from other basins to sustain local water availability, which reflects the vulnerability of freshwater resources in these regions.

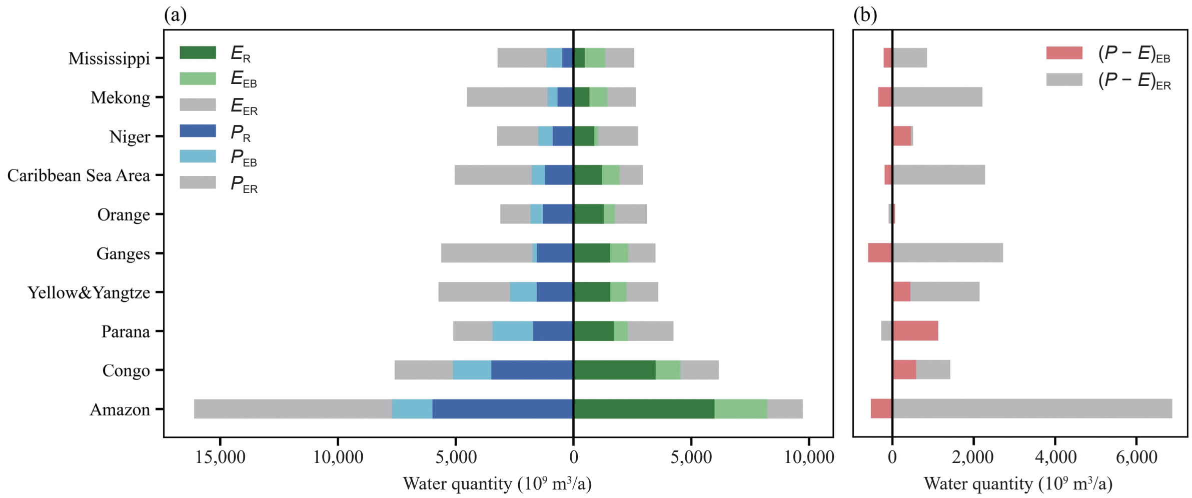

Fig. 5 Green water recycling characteristics of 10 major basins, ranked by green water supplied by the basin. Evapotranspiration and precipitation are divided into their origin and destination in (a): dark green (blue) indicates the total water supplied (received) through terrestrial moisture recycling by the basin itself (E_R and P_R); light green (blue) indicates the water supplied (received) by other basins in the same region (E_{EB} and P_{EB}); gray bars indicate the total water supplied (received) by external regions (E_{ER} and P_{ER}), and the total length of the bars indicates the total evapotranspiration and precipitation in the basins. The variation of water availability (*P-E*) is subdivided into its origin in (b) similarly with light pink indicating external basin supply and gray indicating external region supply ($(P\text{-}E)_{EB}$ and $(P\text{-}E)_{ER}$).

4 Conclusions and implications

Our results show that basins are far from being independent systems, in contrast to common notions based on a terrestrial perspective of hydrology, as they have extensive green water exchange with adjacent basins and the ocean through the atmosphere. Using the Lagrangian moisture model, we assess the global green water recycling network at the continental and basin scales. For large continents, green water is mainly transported to the region itself and the surrounding ocean. When basins are further considered, green water from a specific basin supports precipitation not only within the basin but also in nearby basins and even distant areas, which implies independence and connectivity among basins. Large basins like the Amazon and Congo were found to be much more independent with green water ratio reaching 61.5% and 56.6%, while at the same time acting as important moisture suppliers to other basins. Smaller basins such as Parana and Nile show a higher dependence on external moisture sources with 33.7% and 27.5% of precipitation contributed by surrounding basins, respectively. Cross-basin green water flows are usually controlled by the predominant wind with source basins in the upwind and sink basins in the downwind. Specifically, our analysis highlights that the prevailing trade winds drive the moisture exchange in tropical basins like the San Francisco and Nile, whereas the intense cross-basin transport in North America and Europe is predominantly governed by the westerly winds. Besides, the existence of cascading moisture recycling among several basins induces even more intensive green water exchange. Nevertheless, even the basins with the largest green water flow remain dependent on the moisture supplied by other basins to some extent, and an imbalance in this atmospheric exchange of water between basins can be detected, which may further impact the water availability. Therefore, the natural green water cross-basin transport process has a significant impact on the patterns of water resource distribution.

This assessment, based on climatological data, reflects average historical conditions shaped by atmosphericcirculation, regional climate, and land use. Future climate change could alter regional climatic conditions and large-scale atmosphericcirculation. Simultaneously, human activities could significantly impact land use, thus influencing evaporation and green water dynamics.However, precise modeling of future moisture trajectories is challenging due to inherent uncertainties in global climate models, whichcannot provide reliable input fields for future moisture tracking. Consequently, research on future global green water recycling patternsremains limited, requiring further exploration. While some studies evaluate the potential hydrological effects of forestation throughmoisture recycling, often assuming that recycling patterns remain unchanged despite potential land cover shifts (Cui et al., 2022; Hoek van Dijke et al., 2022), an assumption that warrants refinement. Future research should focus on predicting green water recycling adjustments,especially in key basins such as Amazon, Yangtze, and Tibetan Plateau, which are critical for both local and global watermanagement.

These results emphasize the importance of considering green water as a source of precipitation and freshwater availability. Therefore, to achieve a complete assessment of freshwater vulnerability, the impacts of upwind evapotranspiration should be taken into account as an important supplier of precipitation downwind. Further, large-scale human activities, such as land use changes or irrigation, can cause green water changes that spread downwind through atmospheric moisture recycling, and consequently affect water management of freshwater availability in nearby basins. Similarly, water scarcity and droughts may also propagate from basin to basin as a result of the decreased green water in the source region. These processes strongly depend on large-scale atmospheric circulation and land-atmosphere feedback, proving once again that freshwater scarcity and sustainable water usage are global challenges that shouldn't be constrained by geographic and political boundaries. The water planetary boundary framework proposed by Gleeson et al. (2020) and Zipper et al. (2020) points out that water resource governance needs to take into account the water cycle across basin scales, and integrate with land and climate change by relying on the hydrological linkages across basin scales, considering the blue water, green water, and frozen water resources. Our research provides a comprehensive perspective of the global green water recycling network, thus providing a reference to integrate green water into the framework of the water planetary boundary.

Data availability

The HydroBASINS dataset is obtained from https://www.hydrosheds.org/products/hydrobasins. The ERA-Interim data were obtained from http://apps.ecmwf.int/datasets (closed on June 1st, 2023). The LAGRANTO source code can be downloaded from www.lagranto.ethz.ch and the UTrack model code is available at https://github.com/ObbeTuinenburg/UTrack-atmospheric-moisture.

Declaration of competing interests

The authors have no competing interests to declare that are relevant to the content of this article. The author Guangqian Wang is the Editor-in-Chief of this journal. The author Deyu Zhong is the member of Acting Executive Editor of this journal.

References

Alcamo, J., Henrichs, T. (2002). Critical regions: a model-based estimation of world water resources sensitive to global changes. *Aquatic Sciences*, 64: 352–362

Cui, J. P., Lian, X., Huntingford, C., Gimeno, L., Wang, T., Ding, J. Z., He, M. Z., Xu, H., Chen, A. P., Gentine, P., et al. (2022). Global water availability boosted by vegetation-driven changes in atmospheric moisture transport. *Nature Geoscience*, 15: 982–988

Dee, D. P., Uppala, S. M., Simmons, A. J., Berrisford, P., Poli, P., Kobayashi, S., Andrae, U., Balmaseda, M. A., Balsamo, G., Bauer, P., et al. (2011). The ERA-Interim reanalysis: configuration and performance of the data assimilation system. *Quarterly Journal of the Royal Meteorological Society*, 137: 553–597

Falkenmark, M., Lundqvist, J., Widstrand, C. (1989). Macro-scale water scarcity requires micro-scale approaches. *Natural Resources Forum*, 13: 258–267

Falkenmark, M., Rockström, J. (2006). The new blue and green water paradigm: breaking new ground for water resources planning and management. *Journal of Water Resources Planning and Management*, 132: 129–132

Falkenmark, M., Wang-Erlandsson, L., Rockström, J. (2019). Understanding of water resilience in the Anthropocene. *Journal of Hydrology X*, 2: 100009.

Flörke, M., Schneider, C., McDonald, R. I. (2018). Water competition between cities and agriculture driven by climate change and urban growth. *Nature Sustainability*, 1: 51–58

Gerten, D., Heinke, J., Hoff, H., Biemans, H., Fader, M., Waha, K. (2011). Global water availability and requirements for future food production. *Journal of Hydrometeorology*, 12(5): 885–899.

Gimeno, L., Vázquez, M., Eiras-Barca, J., Sorí, R., Stojanovic, M., Algarra, I., Nieto, R., Ramos, A. M., Durán-Quesada, A. M., Dominguez, F. (2020). Recent progress on the sources of continental precipitation as revealed by moisture transport analysis. *Earth-Science Reviews*, 201: 103070.

Gleeson, T., Wang-Erlandsson, L., Zipper, S. C., Porkka, M., Jaramillo, F., Gerten, D., Fetzer, I., Cornell, S. E., Piemontese, L., Gordon, L. J., et al. (2020). The water planetary boundary: interrogation and revision. *One Earth*, 2: 223–234

Hoek van Dijke, A. J., Herold, M., Mallick, K., Benedict, I., Machwitz, M., Schlerf, M., Pranindita, A., Theeuwen, J. J. E., Bastin, J. F., Teuling, A. J. (2022). Shifts in regional water availability due to global tree restoration. *Nature Geoscience*, 15(5): 363–368.

Keune, J., Miralles, D. G. (2019). A precipitation recycling network to assess freshwater vulnerability: challenging the watershed convention. *Water Resources Research*, 55(11): 9947–9961.

Keys, P. W., Wang-Erlandsson, L., Gordon, L. J., Galaz, V., Ebbesson, J. (2017). Approaching moisture recycling governance. *Global Environmental Change*, 45: 15–23.

Keys, P. W., Wang-Erlandsson, L., Gordon, L. J. (2018). Megacity precipitationsheds reveal tele-connected water security challenges. *PLoS One*, 13: e0194311

Kummu, M., Ward, P. J., De Moel, H., Varis, O. (2010). Is physical water scarcity a new phenomenon? Global assessment of water shortage over the last two millennia. *Environmental Research Letters*, 5: 034006

Kummu, M., Gerten, D., Heinke, J., Konzmann, M., Varis, O. (2014). Climate-driven interannual variability of water scarcity in food production potential: a global analysis. *Hydrology and Earth System Sciences*, 18: 447–461

Lehner, B., Grill, G. (2013). Global River hydrography and network routing: baseline data and new approaches to study the world's large river systems. *Hydrological Processes*, 27: 2171–2186

Lehner, B., Verdin, K., Jarvis, A. (2008). New global hydrography derived from spaceborne elevation data. *Eos, Transactions American Geophysical Union*, 89: 93–94

Li, Y., Xu, R., Yang, K., Liu, Y. X., Wang, S., Zhou, S., Yang, Z., Feng, X. M., He, C. Y., Xu, Z. J., et al. (2023). Contribution of Tibetan Plateau ecosystems to local and remote precipitation through moisture recycling. *Global Change Biology*, 29: 702–718

Liu, J. G., Zehnder, A. J. B., Yang, H. (2009). Global consumptive water use for crop production: the importance of green water and virtual water. *Water Resources Research*, 45: W05428

Liu, J. G., Yang, H., Gosling, S. N., Kummu, M., Flörke, M., Pfister, S., Hanasaki, N., Wada, Y., Zhang, X. X., Zheng, C. M., et al. (2017). Water scarcity assessments in the past, present, and future. *Earth's Future*, 5: 545–559

Meier, R., Schwaab, J., Seneviratne, S. I., Sprenger, M., Lewis, E., Davin, E. L. (2021). Empirical estimate of forestation-induced precipitation changes in Europe. *Nature Geoscience*, 14: 473–478

Mekonnen, M. M., Hoekstra, A. Y. (2011). The green, blue and grey water footprint of crops and derived crop products. *Hydrology and Earth System Sciences*, 15: 1577–1600

Mekonnen, M. M., Hoekstra, A. Y. (2016). Four billion people facing severe water scarcity. *Science Advances*, 2: e1500323

Miralles, D. G., Gentine, P., Seneviratne, S. I., Teuling, A. J. (2019). Land-atmospheric feedbacks during droughts and heatwaves: state of the science and current challenges. *Annals of the New York Academy of Sciences*, 1436: 19–35

Oki, T., Kanae, S. (2006). Global hydrological cycles and world water resources. *Science*, 313: 1068–1072

Rockström, J., Steffen, W., Noone, K., Persson, Å., Chapin, F. S., Lambin, E. F., Lenton, T. M., Scheffer, M., Folke, C., Schellnhuber, H. J., et al. (2009). A safe operating space for humanity. *Nature*, 461: 472–475

Rockström, J., Mazzucato, M., Andersen, L. S., Fahrländer, S. F., Gerten, D. (2023). Why we need a new economics of water as a common good. *Nature*, 615: 794–797

Schär, C., Lüthi, D., Beyerle, U., Heise, E. (1999). The soil–precipitation feedback: a process study with a regional climate model. *Journal of Climate*, 12: 722–741

Seneviratne, S. I., Corti, T., Davin, E. L., Hirschi, M., Jaeger, E. B., Lehner, I., Orlowsky, B., Teuling, A. J. (2010). Investigating soil moisture–climate interactions in a changing climate: a review. *Earth-Science Reviews*, 99: 125–161

Spracklen, D. V., Arnold, S. R., Taylor, C. M. (2012). Observations of increased tropical rainfall preceded by air passage over forests. *Nature*, 489: 282–285

Sprenger, M., Wernli, H. (2015). The LAGRANTO Lagrangian analysis tool–version 2. *0. Geoscientific Model Development*, 8: 2569–2586

Sterling, S. M., Ducharne, A., Polcher, J. (2013). The impact of global land-cover change on the terrestrial water cycle. *Nature Climate Change*, 3: 385–390

Te Wierik, S. A., Gupta, J., Cammeraat, E. L. H., Artzy-Randrup, Y. A. (2020). The need for green and atmospheric water governance. *WIREs Water*, 7: e1406

Tuinenburg, O. A., Staal, A. (2020a). Tracking the global flows of atmospheric moisture and associated uncertainties. *Hydrology and Earth System Sciences*, 24: 2419–2435

Tuinenburg, O. A., Theeuwen, J. J. E., Staal, A. (2020b). High-resolution global atmospheric moisture connections from evaporation to precipitation. *Earth System Science Data*, 12: 3177–3188

Van der Ent, R. J., Savenije, H. H. G. (2011). Length and time scales of atmospheric moisture recycling. *Atmospheric Chemistry and Physics*, 11: 1853–1863

Wang, G. Q., Zhang, Y., Xie, D., Zhong, D. Y. (2023). Green water in China: geological structure and its significance. *Acta Geographica Sinica*, 78: 1641–1658

Zemp, D. C., Schleussner, C. F., Barbosa, H. M. J., van der Ent, R. J., Donges, J. F., Heinke, J., Sampaio, G., Rammig, A. (2014). On the importance of cascading moisture recycling in South America. *Atmospheric Chemistry and Physics*, 14: 13337–13359

Zemp, D. C., Schleussner, C. F., Barbosa, H. M. J., Hirota, M., Montade, V., Sampaio, G., Staal, A., Wang-Erlandsson, L., Rammig, A. (2017). Self-amplified Amazon forest loss due to vegetation-atmosphere feedbacks. *Nature Communications*, 8: 14681.

Zhang, Y., Huang, W. Y., Zhang, M. X., Tian, Y. L., Wang, G. Q., Zhong, D. Y. (2020). Atmospheric basins: identification of quasi-independent spatial patterns in the global atmospheric hydrological cycle via a complex network approach. *Journal of Geophysical Research: Atmospheres*, 125: e2020JD032796

Zipper, S. C., Jaramillo, F., Wang-Erlandsson, L., Cornell, S. E., Gleeson, T., Porkka, M., Häyhä, T., Crépin, A. S., Fetzer, I., Gerten, D., et al. (2020). Integrating the water planetary boundary with water management from local to global scales. *Earth's Future*, 8: e2019EF001377